1-1-2024

# Simulating compatible solute biosynthesis using a metabolic flux model of the biomining acidophile, acidithiobacillus ferrooxidans ATCC 23270

Himel N. Khaleque
*Edith Cowan University*

Hadi Nazem-Bokaee

Yosephine Gumulya

Ross P. Carlson

Anna H. Kaksonen



10.1016/j.resmic.2023.104115
Khaleque, H. N., Nazem-Bokaee, H., Gumulya, Y., Carlson, R. P., & Kaksonen, A. H. (2024). Simulating compatible solute biosynthesis using a metabolic flux model of the biomining acidophile, acidithiobacillus ferrooxidans ATCC 23270. Research in Microbiology, 175(1-2), article 104115. https://doi.org/10.1016/j.resmic.2023.104115

Research in Microbiology 175 (2024) 104115

Contents lists available at ScienceDirect

Research in Microbiology

journal homepage: www.elsevier.com/locate/resmic

# Simulating compatible solute biosynthesis using a metabolic flux model of the biomining acidophile, *Acidithiobacillus ferrooxidans* ATCC 23270

Himel Nahreen Khaleque [a, b, c, 1, *], Hadi Nazem-Bokaee [b, d, 1], Yosephine Gumulya [a, b, e], Ross P. Carlson [f], Anna H. Kaksonen [a, b]

[a] Commonwealth Scientific and Industrial Research Organisation (CSIRO) Environment, 147 Underwood Avenue, Floreat, WA, Australia
[b] Synthetic Biology Future Science Platform, CSIRO, Canberra 2601, ACT, Australia
[c] School of Science, Edith Cowan University, Joondalup, WA, Australia
[d] Australian National Herbarium, National Research Collections Australia, NCMI, CSIRO, Canberra 2601, ACT, Australia
[e] Centre for Microbiome Research, School of Biomedical Sciences, Queensland University of Technology, Translational Research Institute, Woolloongabba, Queensland, Australia
[f] Center for Biofilm Engineering, Montana State University, Bozeman, MT, USA

ARTICLE INFO

*Article history:*
Received 30 April 2023
Accepted 7 August 2023
Available online 10 August 2023

*Keywords:*
Acidophile
Bioleaching
Compatible solute
Halotolerant
Metabolic flux model

ABSTRACT

Halotolerant, acidophilic, bioleaching microorganisms are crucial to biomining operations that utilize saline water. Compatible solutes play an important role in the adaptation of these microorganisms to saline environments. *Acidithiobacillus ferrooxidans* ATCC 23270, an iron- and sulfur-oxidizing acidophilic bacterium, synthesizes trehalose as its native compatible solute but is still sensitive to salinity. Recently, halotolerant bioleaching bacteria were found to use ectoine as their key compatible solute. Previously, bioleaching bacteria were recalcitrant to genetic manipulation; however, recent advancements in genetic tools and techniques allow successful genetic modification of *A. ferrooxidans* ATCC 23270. Therefore, this study aimed to test, *in silico*, the effect of native and synthetic compatible solute biosynthesis by *A. ferrooxidans* ATCC 23270 on its growth and metabolism. Metabolic network flux modelling was used to provide a computational framework for the prediction of metabolic fluxes during production of native and synthetic compatible solutes by *A. ferrooxidans* ATCC 23270, *in silico*. Complete pathways for trehalose biosynthesis by the bacterium are proposed and captured in the updated metabolic model including a newly discovered UDP-dependent trehalose synthesis pathway. Finally, the effect of nitrogen sources on compatible solute production was simulated and showed that using nitrogen gas as the sole nitrogen source enables the ectoine-producing 'engineered' microbe to oxidize up to 20% more ferrous iron in comparison to the native microbe that only produces trehalose. Therefore, the predictive outcomes of the model have the potential to guide the design and optimization of a halotolerant strain of *A. ferrooxidans* ATCC 23270 for saline bioleaching operations.



## 1. Introduction

Biomining (or bioleaching) is the process of extracting metals from low grade mineral ores using microbes that oxidize iron and/or sulfur at low pH; i.e., acidophilic microorganisms [1,2]. Biomining technologies offer advantages over existing technologies for processing low-grade ores as they are less expensive compared to traditional extraction methods such as roasting or smelting [3]. However, high levels of salts, in particular, chloride, in process waters and low-grade mineral ores are toxic to most bioleaching microorganisms [4,5]. Additionally, the high cost of desalination

* Corresponding author. Commonwealth Scientific and Industrial Research Organisation (CSIRO) Environment, 147 Underwood Avenue, Floreat, Western Australia, Australia.
*E-mail addresses:* himelnahreen.khaleque@csiro.au, h.khaleque@ecu.edu.au (H.N. Khaleque), hadi.nazem-bokaee@csiro.au, hadi.nazembokaee@anu.edu.au (H. Nazem-Bokaee), yosephine.gumulya@qut.edu.au (Y. Gumulya), rossc@montana.edu (R.P. Carlson), anna.kaksonen@csiro.au (A.H. Kaksonen).
[1] Himel Nahreen Khaleque and Hadi Nazem-Bokaee contributed equally to this work.

https://doi.org/10.1016/j.resmic.2023.104115

further restricts the use of salt sensitive microorganisms in regions where fresh water is limited or seawater is required for bioleaching operations [4,6,7].

*Acidithiobacillus ferrooxidans* strains are salt-sensitive microbes that are inhibited by >0.2 M sodium chloride [4,8–10]. This limits their use in biomining applications in regions of high salinity. The members of the genus *Acidihalobacter*, however, represent the only known halotolerant (i.e., tolerating high levels of salt) iron- and sulfur-oxidizing acidophiles capable of bioleaching under salt stress, tolerating up to 1.3 M sodium chloride [11–13]. Genomic and proteomic studies of the *Acidihalobacter* spp. have revealed that the production of compatible solutes plays a key role in their halotolerance [11,13]. Compatible solutes, also known as osmoprotectants, are substances that accumulate in the cytoplasm to balance external osmotic pressure while not interfering with the core cellular metabolism [14,15]. They help protect biomining microorganisms and enable them to live in harsh environments of acid, temperature, oxidative, and osmotic stress [15–19]. Trehalose and ectoine are two important compatible solutes produced by acidophilic biomining microorganisms in response to salt stress [20–30]. In a study by Galleguillos et al. [22], trehalose was identified as one of, or the sole, compatible solute in six species of acidophilic bacteria, including *Acidithiobacillus ferrooxidans* strain ILE32, grown at elevated osmotic strength in liquid media. However, to date, trehalose biosynthesis steps have not been fully studied for *A. ferrooxidans* spp. Ectoine accumulation, on the other hand, has been shown to increase halotolerance in *Leptospirillum* and *Acidihalobacter* species [11,31]. In proteomic studies on *Acidihalobacter aeolianus* DSM 14174$^T$, a 422-fold increase was shown in the expression of ectoine synthase at high salt stress [13]. Similarly, in *Acidihalobacter prosperus* DSM 5130$^T$ under salt induced osmotic stress, there was a 50-fold increase in the expression of ectoine transporters [24]. *A. ferrooxidans* ATCC 23270 does not produce ectoine and it has been shown to synthesize trace amounts of trehalose [11,22].

Kaksonen et al., 2020 [32] have previously discussed that engineered microbes are not commonly used in large-scale biomining applications due to regulatory constraints and the lack of technology-ready engineered strains. However, they have also recognized that mining companies are showing increasing interest towards the opportunities synthetic biology can offer and that modelling approaches are gaining popularity as they provide understanding of parameters affecting the growth of bioleaching microorganisms prior to experimental validation [32]. To date, no genetic tools for modification of the *Acidihalobacter* spp. exist. Moreover, the molecular basis of carbon fixation and iron/sulfur oxidation has not yet been published for the *Acidihalobacter* spp. In contrast, *A. ferrooxidans* ATCC 23270 has well-developed genetic tools, and some of its key metabolic capabilities, such as carbon dioxide and nitrogen fixation and iron/sulfur oxidation have been studied comprehensively [33–35]. Furthermore, several metabolic network models have been developed for *A. ferrooxidans* ATCC 23270 providing additional knowledge on carbon dioxide fixation, iron/sulfur oxidation, and extracellular polymeric substances (EPS) production [36–38]. Metabolic flux models have been used extensively over the past two decades for a range of microorganisms and applications such as identifying optimal microbial strains and culture media conditions [39,40], designing metabolic engineering strategies and identifying genetic mutants [41–45], drug targeting and production of chemicals [46], and creating databases/knowledgebases of biochemical and genetic information [47–55]. However, this powerful computational systems biology approach has rarely been realized for the exploration of the metabolic capabilities of biomining microorganisms such as compatible solute biosynthesis.

In this study, we aim at extending the application of genome-scale metabolic flux modelling for the examination of different plausible native trehalose biosynthetic routes as well as a synthetic ectoine biosynthesis pathway by *A. ferrooxidans* ATCC 23270. Such computational framework allows for better understanding the interplay of trehalose and ectoine biosynthesis with respect to the growth and metabolism of *A. ferrooxidans* ATCC 23270. We build upon existing data by extending a currently existing metabolic model, iMC507 [38], of *A. ferrooxidans* ATCC 23270 to include the pathways, reactions, proteins and metabolites required for the biosynthesis of the compatible solutes trehalose and ectoine. This updated metabolic model of *A. ferrooxidans* ATCC 23270 was used to predict the theoretical limits of native trehalose and non-native ectoine biosynthesis yields. We also performed a detailed flux analysis to compare key differences between a trehalose-producing acidophile versus a potentially engineered ectoine-producing acidophile at metabolite level, *in silico*.

## 2. Methods

### 2.1. Model assembly

Using the iMC507 genome-scale metabolic model of *A. ferrooxidans* ATCC 23270 [38] as the base model, the updated metabolic model of *A. ferrooxidans* ATCC 23270 was constructed by adding genes and reactions enabling trehalose and ectoine biosynthesis to the base model. To simulate ectoine biosynthesis by the bacterium, four new reactions and eight genes borrowed from *Acidihalobacter* spp. were added to the original iMC507 model [11]. These include a diaminobutyrate pyruvate aminotransferase (EctA), a L-2,4-diaminobutyric acid acetyltransferase (EctB), a L-ectoine synthase (EctC) [56], and an ectoine exchange reaction (to allow for ectoine exchange with the extracellular environment). Also, we performed an in-depth search for the possible routes of trehalose biosynthesis in both the sequenced annotated genome of *A. ferrooxidans* ATCC 23270, as well as in the literature. In total, six new reactions and eight genes were added to the updated model allowing for the formation of trehalose through both ADP-dependent and UDP-dependent TreT pathway, as well as via the TreY-TreZ pathway. *In silico* production of the osmoprotectants trehalose and ectoine, therefore, simulates the metabolism of *A. ferrooxidans* ATCC 23270 under high salt concentrations.

We also revised glycogen biosynthesis and degradation pathways used by *A. ferrooxidans* ATCC 23270 in the updated metabolic model because the previous models of the bacterium, which focused mainly on EPS biosynthesis, provided partial information on glycogen metabolism. We assumed that the degree of polymerization of 1,4-alpha-glucan (glycogen) branching enzyme (2.4.1.18) equals to six, and the enzyme transfers glycosyl groups to a monomer with similar formula as amylose (i.e., debranched glycogen). The glycogen, produced by glycogen branching enzyme, is consequently utilized by either a glycogen phosphorylase (GlgP) or an alpha amylase (Amy). Glycogen phosphorylase phosphorylates and converts glycogen into two glucose-1-phosphate and one maltotetraose, while alpha amylase hydrolyzes two molecules of glycogen into maltotetraose.

Next, all reactions of the updated model were charge- and mass-balanced leading to the identification of four reactions with incorrect stoichiometric coefficients in the iMC507 model. This included a periplasmic sodium–calcium antiporter, a sodium-proton antiporter, 1,4-alpha-glucan branching enzyme, and glycogen phosphorylase. Additionally, the directionality of seven reactions were corrected according to the thermodynamic data available for those reactions in the MetaCyc database [57]. This included changing the following reactions to run irreversibly:

acetyl-CoA carboxylase, glucokinase, CTP synthase (glutamine hydrolysing), glycogen phosphorylase, maltodextrin phosphorylase, and sedoheptulose-bisphosphatase.

As a result of new pathway additions, seven new metabolites were also introduced to the base metabolic network of *A. ferrooxidans* ATCC 23270. Chemical formulae of glycogen was changed to $(C_{12}H_{20}O_{10})_n$ where n = 3. This enabled accounting for phosphorylation of glycogen to maltotetraose and glucose-1-phosphate by glycogen phosphorylase (EC: 2.4.1.1) to provide the substrate of malto-oligosyltrehalose synthase (EC: 5.4.99.15), which acts on maltodextrins having a polymerisation degree higher than three [58]. The full list of new and revised reactions and metabolites is available in Tables S1 and S2 of the supplementary file.

### 2.2. Growth and product formation predictions

The updated metabolic model of *A. ferrooxidans* ATCC 23270 was named iATF-ENG to follow the existing conventions [59]. The textual format of the model is available as an Excel file (Table S1 of the Supplementary file). All reaction fluxes are in mmol/gDCW-h except for the reaction representing cell biomass formation that is expressed in $h^{-1}$. The medium composition was assumed to be minimal medium [38]. The model was assembled in a format compatible for flux balance analysis (FBA) [60]. FBA optimization problems were solved by both the GNU Linear Programming Kit (GLPK) solver (http://www.gnu.org/software/glpk/) and built-in MATLAB solver in MATLAB using COBRA toolbox [61].

To simulate growth of *A. ferrooxidans* ATCC 23270 using the iATF-ENG model, bicarbonate assimilation rate was fixed to 1 mmol/gDCW.h, and the uptake of oxygen, phosphorous, nitrogen, sulfur, and metal ions were left unbounded. Additionally, transport of proton and water across the *in silico* cell membrane were left unconstrained. The objective function of the FBA optimization problem was maximisation of biomass, trehalose, or ectoine production. In addition to ectoine and trehalose as the target products of *in silico* growth of *A. ferrooxidans* ATCC 23270, exopolysaccharide and glucose were considered as by-products, and allowed to leave the system (i.e., to be exported into the extracellular environment if needed). Non-growth associated maintenance ATP was set to 3.475 mmol/gDCW.h as described previously [38].

## 3. Results and discussion

The updated iATF-ENG metabolic model developed in this study contains 631 reactions, 580 metabolites, and 515 genes (Supplementary file, Tables S1 and S2). Ten new reactions were added to enable trehalose or ectoine biosynthesis. Additionally, nine reactions were corrected for mass or charge imbalances. The first stoichiometric model of a bioleaching microorganism was that of *A. ferrooxidans* ATCC 23270 published by Hold et al. [36], in which only 62 reactions were used. While the model was able to simulate values of maximum oxygen uptake similar to experimental values, the study assumed a complete tricarboxylic acid (TCA) cycle and included all the reactions and metabolites of the complete TCA cycle in the model. However, *A. ferrooxidans* is known to have an incomplete TCA cycle as genes encoding E1-3 subunits of α-ketoglutarate dehydrogenase are absent from its genome [62]. This absence of a complete TCA cycle has been suggested to be a hallmark of the obligate autotrophic lifestyle of this acidophile, therefore, the inclusion of the entire cycle could lead to incorrect predictions of metabolism [62]. The second model for *A. ferrooxidans* ATCC 23270, published by Sepúlveda [37], updated the previous model to remove the extra reactions of the TCA cycle and to include a total of 190 reactions, 100 exclusively related to biomass production, 20 involved in central metabolism and energy generation and the remaining associated to extracellular polymeric substances (EPS) synthesis. This model was able to show that the disruption of the incomplete TCA cycle leads to overproduction of EPS. More recently, a comprehensive model of *A. ferrooxidans* ATCC 23270, iMC507, was generated which included reaction information from 507 open reading frames [38]. Expanding on studies of EPS production by Sepúlveda [37], the iMC507 model helped to further study growth coupled EPS production and validate the presence of malate dehydrogenase (MDH) and fumarase (FUM) reactions in the incomplete TCA cycle. However, while trehalose is natively synthesized by *A. ferrooxidans* ATCC 23270, the pathway for its synthesis was neither captured in the iMC507 metabolic model nor in any of the previous metabolic models of *A. ferrooxidans* ATCC 23270. The updated iATF-ENG model captures all the recent amendments described above. The inclusion of the synthetic ectoine biosynthesis pathway, updating glycogen metabolism, and updating trehalose biosynthetic pathways did not alter the simulated values obtained for the growth of wild-type *A. ferrooxidans* ATCC 23270 as predicted by the iMC507 metabolic model.

### 3.1. Prediction of growth and product formation by the iATF-ENG updated metabolic model of A. ferrooxidans

The maximum biomass yield predicted by the iATF-ENG model is 0.026 g per mole bicarbonate, which is identical to the value predicted by the iMC507 model, confirming that the addition of synthetic pathways or updating the trehalose biosynthesis pathways did not impact growth predictions. The iATF-ENG model of *A. ferrooxidans* ATCC 23270 supports the biosynthesis of both native (trehalose) and engineered (ectoine) compatible solutes. On a mole basis, the maximum theoretical production yields of trehalose and ectoine reaches to, respectively, 0.083 and 0.166 mol per mole bicarbonate (Fig. 1) as the sole carbon source (i.e., assuming that all incoming carbon is converted into trehalose or ectoine and no biomass is formed). When the production of both ectoine and trehalose was shut down (i.e., constraining the bounds of exchange reactions of both ectoine and trehalose to zero), the incoming carbon was converted into EPS. The maximum EPS yield (at no growth) was reached to 0.108 mol EPS per mole bicarbonate.

*A. ferrooxidans* ATCC 23270 can meet its nitrogen needs by either nitrogen fixation or ammonia assimilation. Valdes et al. [62] have depicted a genomic model for nitrogen fixation through the nitrogenase operon as well as a model for ammonia uptake. The iAFT-ENG model also supports growth with both ammonia and nitrogen gas, *in silico*. Fig. 1 shows predicted growth as a function of nitrogen uptake (as nitrogen gas molecule) per mole of incoming carbon source. Based on Fig. 1, both ectoine and trehalose production are growth-uncoupled (i.e., they compete with cellular growth). The iATF-ENG model predicted increased flux through fumarase, aspartate transaminase, guanosine kinase, guanine phosphoribosyltransferase, malate dehydrogenase, and purine-nucleoside phosphorylase (adenosine) when grown in the presence of ammonia as the nitrogen source. In contrast, when grown with nitrogen gas as the sole source of nitrogen, the fluxes through the oxidative Pentose Phosphate Pathway, folate metabolism, phosphoribulokinase, pyruvate kinase, phosphoserine transaminase, phosphoserine phosphatase, nitrogenase, malate synthase and glycolysis were elevated.

### 3.2. Analysis of compatible solute biosynthesis — a comparison between trehalose and ectoine biosynthesis pathways based on flux-balanced predictions

Bacterial trehalose can be synthesized by 4 different pathways. The most common route of trehalose synthesis is through the

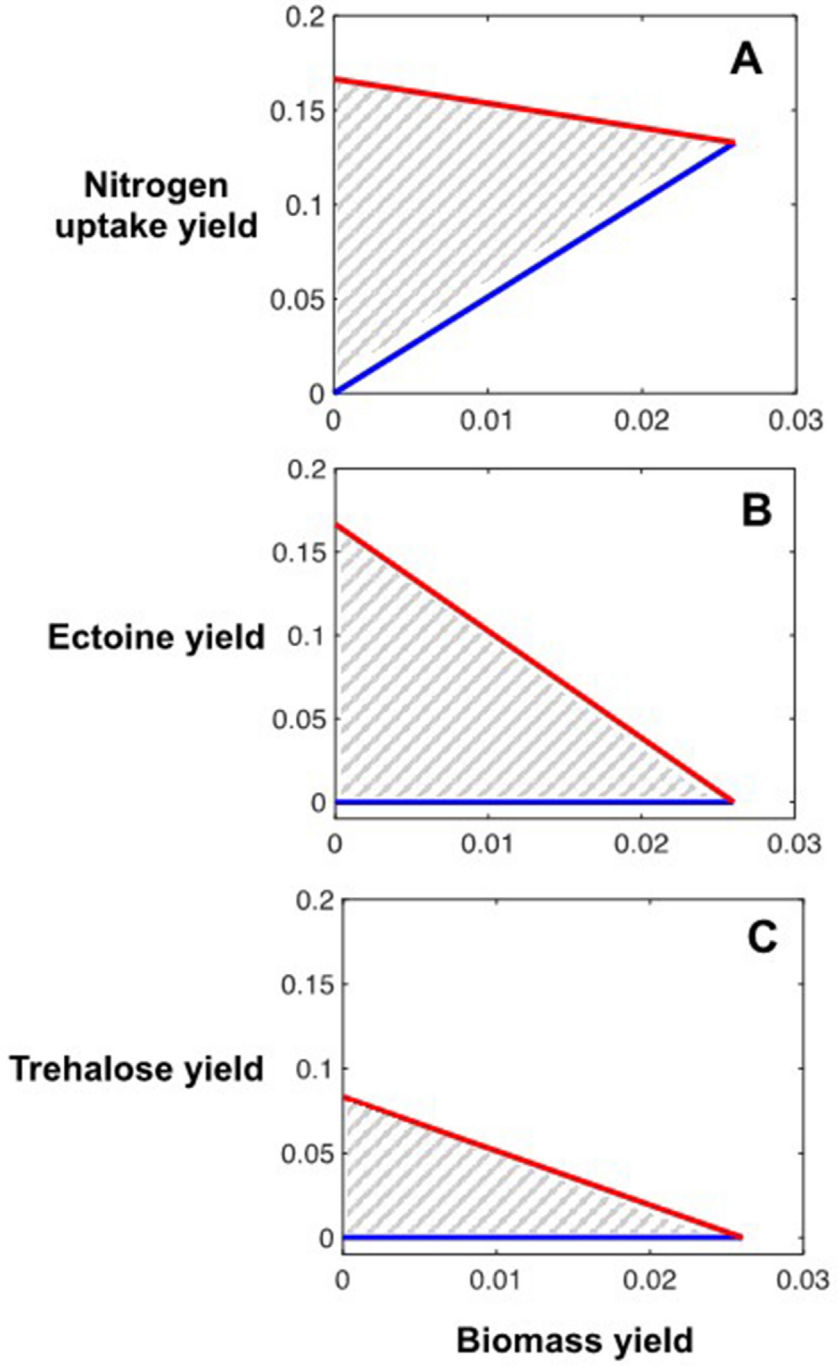


**Fig. 1.** Production envelopes showing predicted interplay between growth (as biomass yield) of *A. ferrooxidans* ATCC 23270 and uptake of nitrogen (as nitrogen gas molecule) (A), ectoine production (B), and trehalose production (C). The shaded areas represent the feasible solution space predicted by the iATF-ENG model. All yields are in mole per mole of carbon dioxide except for the biomass, which is grams biomass per mole carbon dioxide. Red and blue lines indicate, respectively, the upper and lower limits of theoretically feasible yields. (For interpretation of the references to color in this figure legend, the reader is referred to the Web version of this article.)

OtsAB pathway, catalyzed by trehalose-6-phosphate synthase (OtsA) and trehalose-6-phosphatase (OtsB) [63]. This proceeds from UDP-glucose and glucose-6-phosphate to form trehalose-6-phosphate, which is dephosphorylated to yield free trehalose. Secondly, in the TreS (trehalose synthase) pathway, trehalose is formed by the transglycosylation of maltose [63,64]. The third pathway is through TreYZ in which the substrates are oligomaltodextrin or glycogen [63]. Here, TreY (maltooligosyl trehalose synthase) transglycosylates a terminal maltosyl residue into a trehalosyl residue, which then liberates trehalose by the activity of TreZ (maltooligosyl trehalose hydrolase) [63]. Finally, and more recently, the hyperthermophilic archaeon *Thermococcus litoralis*, was found to contain a trehalose synthesizing enzyme called TreT. In the TreT pathway, ADP(UDP/GDP)-glucose and glucose are converted to trehalose through the action of trehalose glycosyltransferring synthase (TreT) [65]. The genome of *A. ferrooxidans* ATCC 23270 was found to contain genes coding for the TreT and TreYZ pathway proteins for trehalose synthesis but not for TreS or OtsAB

pathway proteins. This is interesting, because the TreYZ pathways are much less prominent in bacteria [63,66]. More so, the TreT pathway is relatively new and to date has only been found in a few archaeal (e.g., *Thermococcales*) and bacterial (*Thermotogales*) members [65,67]. Furthermore, previously it was hypothesized that *A. ferrooxidans* can only produce trehalose through the TreT-ADP pathway [68]. However, in *T. litoralis*, the TreT pathways was shown to have the highest activity on ADP-glucose but could also use UDP- or GDP-glucose [65]. The genome of *A. ferrooxidans* ATCC 23270 was also found to possess the genes encoding UTP-glucose-1-phosphate uridylyltransferase and a UDP-dependent trehalose glycosyltransferring synthase.

In this study, three simulations were run to simulate trehalose biosynthesis through each of the three pathways (depicted in Fig. 2). For simulating trehalose biosynthesis via the TreYZ pathway, both TreT1 and TreT2 reactions were inactivated (i.e., both lower and upper bounds of the reactions were set to zero). Here, TreT1 reaction refers to the ADP-dependent TreT and TreT2 reaction refers to the UDP-dependent TreT. Likewise, for simulating trehalose biosynthesis via ADP-dependent TreT pathway, both TreT2 and

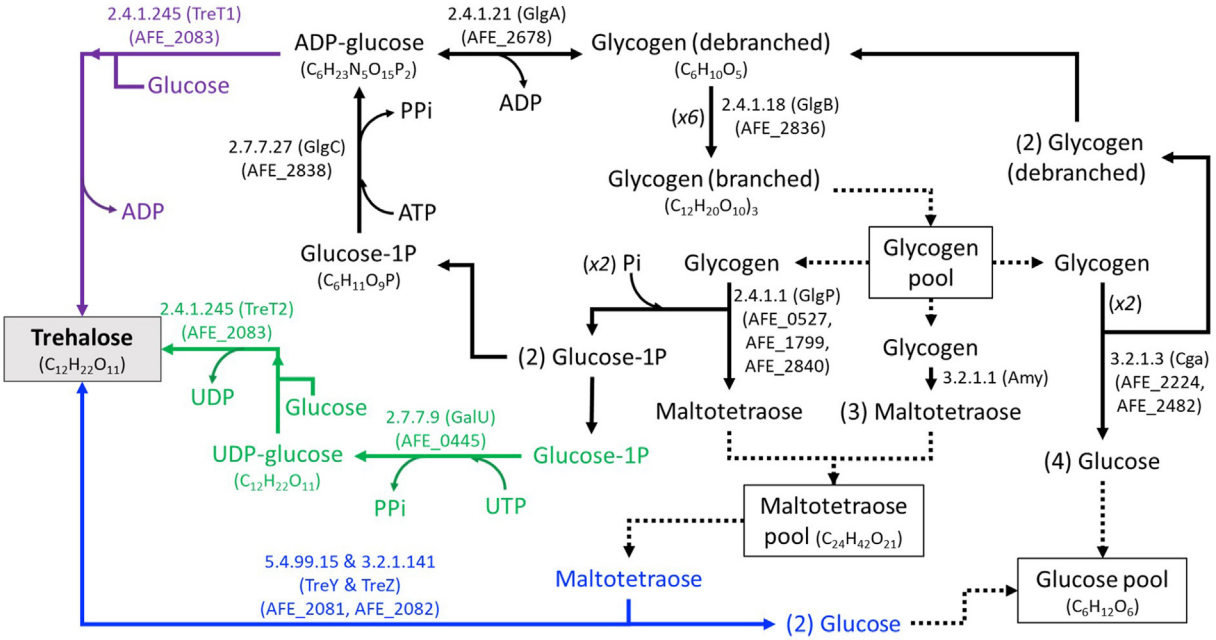


**Fig. 2.** Proposed trehalose biosynthesis pathways for *A. ferrooxidans* ATCC 23270. Steps involved in ADP-dependent TreT, UDP-dependent TreT, and TreYZ pathways are shown in purple, green, and blue colours, respectively. Steps in black show glycogen biosynthesis and degradation pathways. Steps shown as dashed lines are for illustrative purposes only. Amy: alpha-amylase (3.2.1.1), Cga: glucoamylase (3.2.1.3), GalU: UTP-glucose-1-phosphate uridylyltransferase (2.7.7.9), GlgA: debranched glycogen synthase (ADP-dependent) (2.4.1.21), GlgB: 1,4-alpha-glucan branching enzyme (2.4.1.18), GlgC: glucose-1-phosphate adenylyltransferase (2.7.7.27), GlgP: glycogen phosphorylase (2.4.1.1), TreT1: ADP-dependent trehalose glycosyltransferring synthase (2.4.1.245), TreT2: UDP-dependent trehalose glycosyltransferring synthase (2.4.1.245), TreY: malto-oligosyltrehalose synthase (5.4.99.15), TreZ: malto-oligosyltrehalose trehalohydrolase (3.2.1.141). Note that there is no evidence for these pathways to be active simultaneously. (For interpretation of the references to color in this figure legend, the reader is referred to the Web version of this article.)

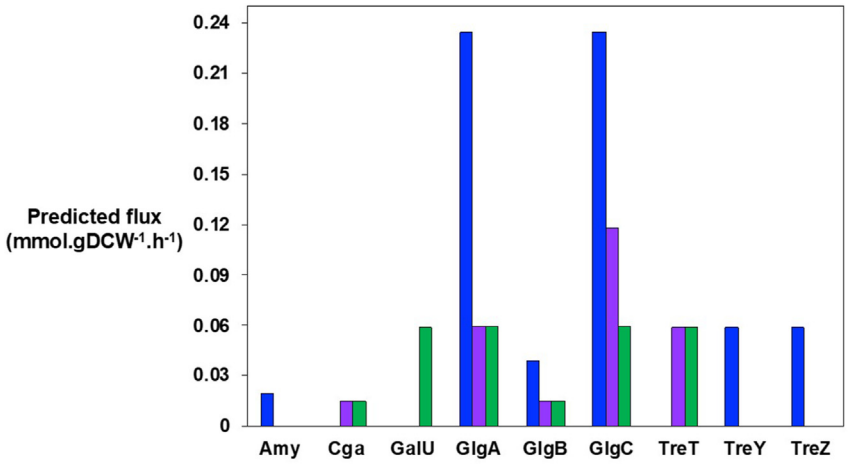


**Fig. 3.** Flux balance analysis of key reactions involved in the biosynthesis of trehalose predicted by the iATF-ENG model of *A. ferrooxidans*. GalU: UTP-glucose-1-phosphate uridylyltransferase (2.7.7.9), GlgA: debranched glycogen synthase (ADP-dependent) (2.4.1.21), GlgB: 1,4-alpha-glucan branching enzyme (2.4.1.18), GlgC: glucose-1-phosphate adenylyltransferase (2.7.7.27), Cga: glucoamylase (3.2.1.3), Amy: alpha-amylase (3.2.1.1), TreY: malto-oligosyltrehalose synthase (5.4.99.15), TreZ: malto-oligosyltrehalose trehalohydrolase (3.2.1.141). Growth rate was fixed to 30% of its maximum. ADP-dependent TreT, UDP-dependent TreT, and TreYZ pathways are shown in purple, green, and blue colours, respectively. (For interpretation of the references to color in this figure legend, the reader is referred to the Web version of this article.)

TreYZ reactions were inactivated; for simulating trehalose biosynthesis via the UDP-dependent TreT pathway, both TreT1 and TreYZ reactions were inactivated.

Flux balance analysis (FBA) results show that all three trehalose biosynthesis pathways shown in Fig. 2 are independently active and support trehalose synthesis (Fig. 3). The results showed that UDP-glucose can also be taken up by trehalose synthase (EC: 2.4.1.245) for trehalose biosynthesis in *A. ferrooxidans* ATCC 23270. Thus, the model supports a novel UDP-dependent trehalose biosynthesis in *A. ferrooxidans* ATCC 23270 in addition to the known ADP-dependent trehalose biosynthesis (TreT) pathway. Based on the flux predictions, shown in Fig. 3, the reaction catalyzed by GlgC

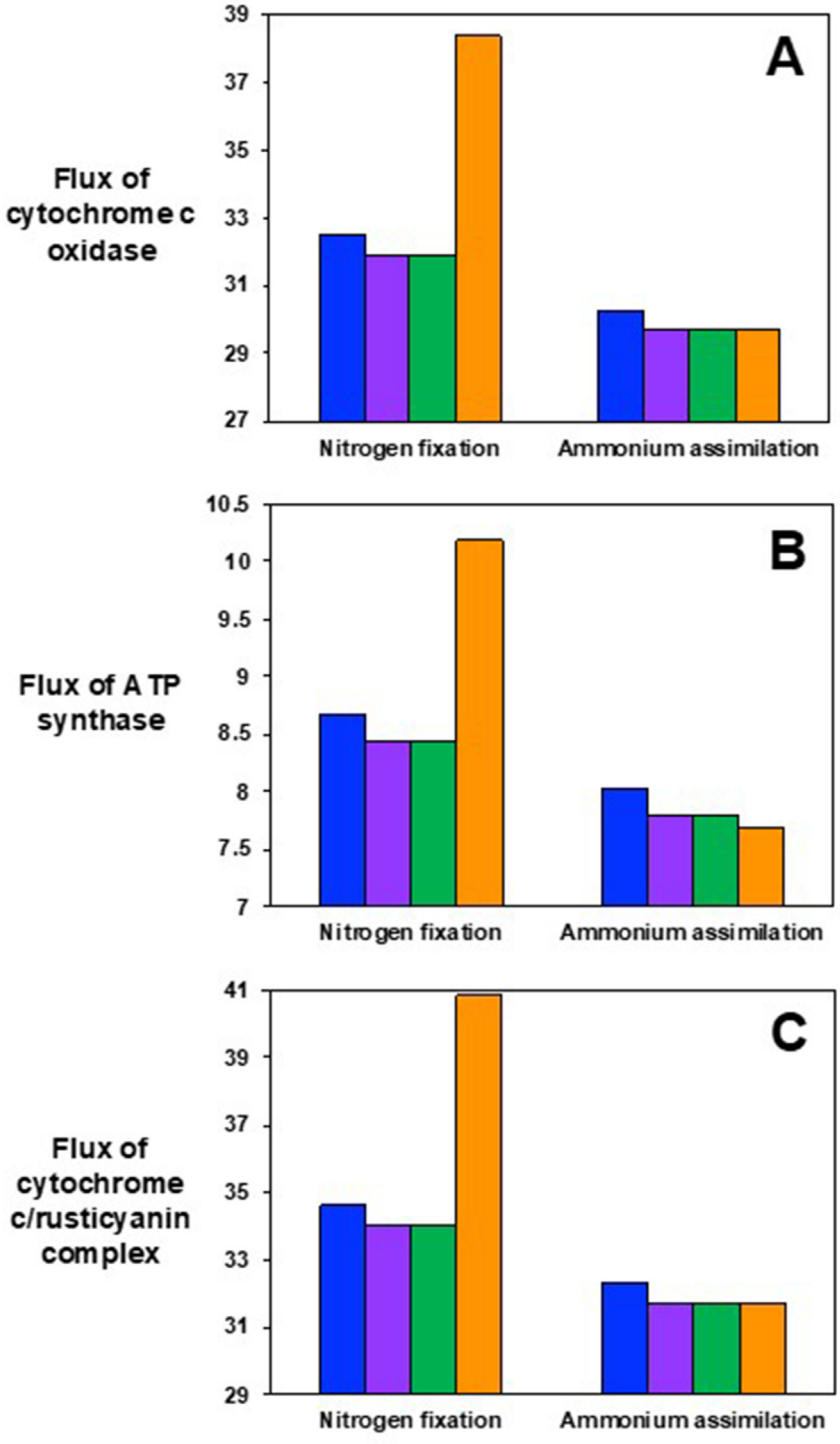


**Fig. 4.** Flux balance analysis showing differences in Fe(II) oxidation (A), ATP generation (B), and oxygen uptake (C) by *A. ferrooxidans* during nitrogen fixation versus ammonia assimilation predicted by the iATF-ENG metabolic model. Growth rate was fixed to 30% of its maximum. Blue: trehalose biosynthesis via ADP-dependent TreT pathway, purple: trehalose biosynthesis via UDP-dependent TreT pathway, green: trehalose biosynthesis via TreYZ pathway, and orange: ectoine biosynthesis pathway. All fluxes shown on Y-axes are in mmol/gDCW.h. (For interpretation of the references to color in this figure legend, the reader is referred to the Web version of this article.)

is the key step in fuelling both TreYZ and ADP-dependent TreT pathways. However, during UDP-dependent trehalose biosynthesis, where both TreYZ and ADP-dependent TreT pathways are inactive, GlgC is still essential. This is because UDP-dependent trehalose synthase requires glucose in addition to UDP-glucose as substrate, and the only way *A. ferrooxidans* ATCC 23270 can provide glucose demand is by synthesising glycogen (via GlgC and GlgA) and further breaking it down to glucose (via GlgB and Cga). The UDP-dependent TreT pathway requires less ATP input for trehalose biosynthesis compared with TreYZ and ADP-dependent TreT pathways according to the model predictions. In other words, based on the flux data predicted by the iATF-ENG model, trehalose yield (mole trehalose produced per mole ATP consumed) is 0.98 when trehalose is synthesized through the UDP-dependent TretT pathway. However, trehalose yield reduces to 0.49 and 0.25 when trehalose is synthesised through the ADP-dependent TretT and TreYZ pathways, respectively. This translates to 50.2% higher flux through the reaction catalyzed by GlgC (shown in Fig. 3) via the ADP-dependent TreT pathway than via the UDP-dependent TreT pathway, and 74.6% higher via the TreYZ pathway than via the UDP-dependent TreT pathway. Selecting UDP-dependent TreT pathway could be an adaptation mechanism for *A. ferrooxidans* under stress (for example, at high salt concentrations), where cells must balance ATP resources for both survival (biomass formation) and stress tolerance (trehalose biosynthesis). Further experimental validations are needed to justify such hypothesis.

The iATF-ENG model predictions suggest that *A. ferrooxidans* growing with nitrogen gas (as the sole nitrogen source) oxidizes 7.3% up to 29.2% more Fe(II) compared to its growth with ammonia as the sole nitrogen source (Fig. 4A). The engineered strain growing with nitrogen gas (as the sole nitrogen source) and producing ectoine oxidizes up to 20% more Fe(II) compared with the strain producing trehalose (Fig. 4A). According to the flux data predicted by the iATF-ENG model, nitrogen fixation by nitrogenase generates dihydrogen gas that *A. ferrooxidans* dissipates through a quinone-dependent hydrogenase. The conversion of dihydrogen to protons increases the proton gradient across the membrane, and therefore, increases flux through the oxidative phosphorylation pathway. The generation of additional electrons during nitrogen fixation (compared to ammonia assimilation) along with increased proton gradient results in increased flux through the ATP synthase (Fig. 4B), and increased flux through cytochrome c/rusticyanin complex, which transfers the electrons to oxygen as the terminal electron acceptor (Fig. 4C). These results suggest that engineering *A. ferrooxidans* to produce the non-natural compatible solute ectoine could be a promising option for generating halotolerant strain.

## 4. Conclusions

Systems and synthetic biology offer new opportunities for engineering microbes to adapt to a range of extreme environmental conditions during bioleaching operations. However, there is a lack of a systems-level understanding of metabolic interactions in such complex systems. In this work, we introduced an updated genome-scale metabolic flux model of the acidophile *A. ferrooxidans* ATCC 23270 enabling the prediction of metabolic interplay between compatible solute biosynthesis and the growth of the bacterium. Biosynthesis of trehalose (a native compatible solute) and ectoine (a heterologous compatible solute) through different metabolic pathways were explored *in silico* which led to the identification of a new UDP-dependent trehalose synthesis route by the bacterium. This computational work does not claim to provide a definite solution to the existing challenges pertaining to high salinity of bioleaching operations. Rather, it presents possible tools and new directions for systems-level engineering of bioleaching microbes that would ultimately lead to more efficient bioleaching processes. The prediction of feasible trehalose biosynthesis via a UDP-dependent trehalose synthase by the iATF-ENG model, for example, introduces a new potential metabolic engineering strategy for increasing the production of native trehalose to assist in improving halotolerance of *A. ferrooxidans* ATCC 23270. The other plausible strategy to improve iron oxidation, and therefore metal extraction from mineral ores, is to engineer *A. ferrooxidans* to produce ectoine while growing the engineered microbe with nitrogen gas as the sole source of nitrogen. Nonetheless, some of the potential areas for future development and/or improvement include (i) updating the biomass equation of the metabolic models for *A. ferrooxidans* since most of the stoichiometric ratios of components in the biomass equation have been borrowed from distantly related bacteria such as *Escherichia coli*, (ii) characterizing rusticyanin chemical composition to better understand its interaction at molecular level with electron donors (e.g., ferrous ions) and electron acceptors (e.g., cytochromes), and (iii) improving low diffusion rates of carbon dioxide to enhance carbon fixation. Furthermore, while in the past acidophilic microorganisms have proven to be recalcitrant to genetic manipulation [69], recent advancements in genetic tools and techniques for *A. ferrooxidans* ATCC 23270 provide more opportunities to engineer this bacterium [70]. For example, recent studies showed that the overexpression of glutathione synthetase in *A. ferrooxidans* ATCC 23270 led to improvements in its ability to tolerate salt stress [35]. Based on the iATF-ENG metabolic mode, glutathione is a component of biomass reaction, and therefore, essential for growth. However, to our best knowledge, there has been no reports on the participation of glutathione in other metabolic pathways of *A. ferrooxidans.* Therefore, new opportunities exist to develop genetically engineered strains of *A. ferrooxidans* ATCC 23270 that would thrive under harsh biomining environments, including salt stress. These tools do not yet exist for halotolerant members of the *Acidihalobacter* genus. Therefore, the updated iATF-ENG metabolic model can serve as a base model and pave the way for developing future computational systems biology tools for studying halotolerance in *Acidihalobacter* species.

## Funding

This research was funded by CSIRO Synthetic Biology Future Science Platform, CSIRO Land and Water, and CSIRO National Collections and Marine Infrastructure (NCMI).

## Author contributions

Conceptualization, H.N.K., H.N.-B., Y.G., and A.H.K.; methodology, H.N.K. and H.N.-B.; software, H.N.-B.; validation, H.N.K. and H.N.-B.; formal analysis, H.N.K. and H.N.-B.; investigation, H.N.K. and H.N.-B.; resources, A.H.K.; data curation, H.N.K. and H.N.-B.; writing—original draft preparation, H.N.K. and H.N.-B.; writing—review and editing, H.N.K., H.N.-B., Y.G., R.C. and A.H.K.; visualization, H.N.K. and H.N.-B.; supervision, A.H.K.; project administration, A.H.K.; funding acquisition, A.H.K. All authors have read and agreed to the published version of the manuscript.

## Declaration of competing interest

The authors declare no conflict of interest.

## Appendix A. Supplementary data

Supplementary data to this article can be found online at https://doi.org/10.1016/j.resmic.2023.104115.

## References


[1] Gómez F. Acidophile. In: Gargaud M, Amils R, Quintanilla JC, Cleaves HJ, Irvine WM, Pinti DL, et al., editors. Encyclopedia of astrobiology. Berlin, Heidelberg: Springer Berlin Heidelberg; 2011. p. 10–2.
[2] Johnson DB. Biomining—biotechnologies for extracting and recovering metals from ores and waste materials. Curr Opin Biotechnol 2014;30:24–31.
[3] Rawlings DE. Characteristics and adaptability of iron-and sulfur-oxidizing microorganisms used for the recovery of metals from minerals and their concentrates. Microb Cell Factories 2005;4:13.
[4] Zammit CM, Watkin ELJ. Adaptation to extreme acidity and osmotic stress. In: Acidophiles: life in extremely acidic environments. UK: Caister Academic Press Norfolk; 2016. p. 49–62.
[5] Kaksonen AH, Boxall NJ, Gumulya Y, Khaleque HN, Morris C, Bohu T, et al. Recent progress in biohydrometallurgy and microbial characterisation. Hydrometallurgy 2018;180:7–25.
[6] Petry M, Sanz MA, Langlais C, Bonnelye V, Durand J-P, Guevara D, et al. The El Coloso (Chile) reverse osmosis plant. Desalination 2007;203:141–52.
[7] Watling H. Microbiological advances in biohydrometallurgy. Minerals 2016;6:49.
[8] Suzuki I, Lee D, Mackay B, Harahuc L, Oh JK. Effect of various ions, pH, and osmotic pressure on oxidation of elemental sulfur by *Thiobacillus thiooxidans*. Appl Environ Microbiol 1999;65:5163–8.
[9] Zammit CM, Mangold S, Jonna V, Mutch LA, Watling HR, Dopson M, et al. Bioleaching in brackish waters—effect of chloride ions on the acidophile population and proteomes of model species. Appl Microbiol Biotechnol 2012;93:319–29.
[10] Gahan CS, Sundkvist J-E, Sandström Å. A study on the toxic effects of chloride on the biooxidation efficiency of pyrite. J Hazard Mater 2009;172:1273–81.
[11] Khaleque HN, González C, Shafique R, Kaksonen A, Holmes DS, Watkin EL. Uncovering the mechanisms of halotolerance in the extremely acidophilic members of the *Acidihalobacter* genus through comparative genome analysis. Front Microbiol 2019;10:155.
[12] Khaleque HN, Kaksonen AH, Boxall NJ, Watkin ELJ. Chloride ion tolerance and pyrite bioleaching capabilities of pure and mixed halotolerant, acidophilic iron- and sulfur-oxidizing cultures. Miner Eng 2018;120:87–93.
[13] Khaleque HN, Shafique R, Kaksonen AH, Boxall NJ, Watkin ELJ. Quantitative proteomics using SWATH-MS identifies mechanisms of chloride tolerance in the halophilic acidophile *Acidihalobacter prosperus* DSM 14174. Res Microbiol 2018;169:638–48.
[14] Kurz M. Compatible solute influence on nucleic acids: many questions but few answers. Saline Syst 2008;4:6.
[15] Empadinhas N, da Costa M. Osmoadaptation mechanisms in prokaryotes: distribution of compatible solutes. Int Microbiol 2008;11:151–61.
[16] Kempf B, Bremer E. Uptake and synthesis of compatible solutes as microbial stress responses to high-osmolality environments. Arch Microbiol 1998:170.
[17] Kindzierski V, Raschke S, Knabe N, Siedler F, Scheffer B, Pflüger-Grau K, et al. Osmoregulation in the halophilic bacterium *Halomonas elongata*: a case study for integrative systems biology. PLoS ONE 2017;12:e0168818.
[18] Roberts MF. Organic compatible solutes of halotolerant and halophilic microorganisms. Saline Syst 2005;1.
[19] Santos H, Da Costa MS. Compatible solutes of organisms that live in hot saline environments. Environ Microbiol 2002;4:501–9.
[20] Galinski EA. Compatible solutes of halophilic eubacteria: molecular principles, water-solute interactions, stress protection. Experientia 1993;49.
[21] Alarico S, Empadinhas N, Simoes C, Silva Z, Henne A, Mingote A, et al. Distribution of genes for synthesis of trehalose and mannosylglycerate in *Thermus* spp. and direct correlation of these genes with halotolerance. Appl Environ Microbiol 2005;71:2460–6.
[22] Galleguillos PA, Grail BM, Hallberg KB, Demergasso CS, Johnson DB. Identification of trehalose as a compatible solute in different species of acidophilic bacteria. J Microbiol 2018;56:727–33.
[23] Calderón MI, Vargas C, Rojo F, Iglesias-Guerra F, Csonka LN, Ventosa A, et al. Complex regulation of the synthesis of the compatible solute ectoine in the halophilic bacterium *Chromohalobacter salexigens* DSM 3043T. Microbiology 2004:150.
[24] Dopson M, Holmes DS, Lazcano M, McCredden TJ, Bryan CG, Mulroney KT, et al. Multiple osmotic stress responses in *Acidihalobacter prosperus* result in tolerance to chloride ions. Front Microbiol 2017;7.
[25] Jebbar M, Sohn-Bösser L, Bremer E, Bernard T, Blanco C. Ectoine-induced proteins in *Sinorhizobium meliloti* include an ectoine ABC-type transporter involved in osmoprotection and ectoine catabolism. J Bacteriol 2005;187:1293–304.
[26] Jebbar M, von Blohn C, Bremer E. Ectoine functions as an osmoprotectant in *Bacillus subtilis* and is accumulated via the ABC-transport system OpuC. Fed Eur Microbiol Soc Microbiol Lett 1997;154:325–30.
[27] Ofer N, Wishkautzan M, Meijler M, Wang Y, Speer A, Niederweis M, et al. Ectoine biosynthesis in *Mycobacterium smegmatis*. Appl Environ Microbiol 2012;78:7483–6.
[28] Robert H, Le Marrec C, Blanco C, Jebbar M. Glycine betaine, carnitine, and choline enhance salinity tolerance and prevent the accumulation of sodium to a level inhibiting growth of *Tetragenococcus halophila*. Appl Environ Microbiol 2000;66:509–17.
[29] Saum SH, Müller V. Regulation of osmoadaptation in the moderate halophile *Halobacillus halophilus*: chloride, glutamate and switching osmolyte strategies. Saline Syst 2008;4:4.
[30] Vargas C, Jebbar M, Carrasco R, Blanco C, Calderón M, Iglesias-Guerra F, et al. Ectoines as compatible solutes and carbon and energy sources for the halophilic bacterium *Chromohalobacter salexigens*. J Appl Microbiol 2006;100:98–107.
[31] Mosier AC, Justice NB, Bowen BP, Baran R, Thomas BC, Northen TR, et al. Metabolites associated with adaptation of microorganisms to an acidophilic, metal-rich environment identified by stable-isotope-enabled metabolomics. mBio 2013;4. e00484-12.
[32] Kaksonen AH, Deng X, Bohu T, Zea L, Khaleque HN, Gumulya Y, et al. Prospective directions for biohydrometallurgy. Hydrometallurgy 2020;195:105376.
[33] Esparza M, Cárdenas JP, Bowien B, Jedlicki E, Holmes DS. Genes and pathways for $CO_2$ fixation in the obligate, chemolithoautotrophic acidophile, *Acidithiobacillus ferrooxidans*, Carbon fixation in *A. ferrooxidans*. BMC Microbiol 2010;10:229.
[34] Quatrini R, Appia-Ayme C, Denis Y, Jedlicki E, Holmes DS, Bonnefoy V. Extending the models for iron and sulfur oxidation in the extreme acidophile *Acidithiobacillus ferrooxidans*. BMC Genom 2009;10:394.
[35] Inaba Y, West AC, Banta S. Glutathione synthetase overexpression in *Acidithiobacillus ferrooxidans* improves halotolerance of iron oxidation. Appl Environ Microbiol 2021;87:e01518–21.
[36] Hold C, Andrews B, Asenjo J. A stoichiometric model of *Acidithiobacillus ferrooxidans* ATCC 23270 for metabolic flux analysis. Biotechnol Bioeng 2009;102:1448–59.
[37] Sepúlveda AEM, Cortéz PAM, Abarca MAB, Valdecantos PAP, Iglesias LMP, Roa MNB. In: Google Patents, editor. Method to increase the production of extracellular polymeric substances (EPS) in an *Acidithiobacillus ferrooxidans* culture by the inhibition of enzymes of tricarboxilic acid cycle; 2011.
[38] Campodonico MA, Vaisman D, Castro JF, Razmilic V, Mercado F, Andrews BA, et al. *Acidithiobacillus ferrooxidans*'s comprehensive model driven analysis of the electron transfer metabolism and synthetic strain design for biomining applications. Metab Eng Commun 2016;3:84–96.
[39] Nazem-Bokaee H, Senger RS. ToMI-FBA: a genome-scale metabolic flux based algorithm to select optimum hosts and media formulations for expressing pathways of interest. Aims Bioeng 2015;2:335–74.
[40] Pharkya P, Burgard AP, Maranas CD. OptStrain: a computational framework for redesign of microbial production systems. Genome Res 2004;14:2367–76.
[41] Burgard AP, Pharkya P, Maranas CD. OptKnock: a bilevel programming framework for identifying gene knockout strategies for microbial strain optimization. Biotechnol Bioeng 2003;84:647–57.
[42] McAnulty MJ, Yen JY, Freedman BG, Senger RS. Genome-scale modeling using flux ratio constraints to enable metabolic engineering of clostridial metabolism *in silico*. BMC Syst Biol 2012;6.
[43] Yen JY, Nazem-Bokaee H, Freedman BG, Athamneh AIM, Senger RS. Deriving metabolic engineering strategies from genome-scale modeling with flux ratio constraints. Biotechnol J 2013;8:581–94.
[44] Ranganathan S, Suthers PF, Maranas CD. OptForce: an optimization procedure for identifying all genetic manipulations leading to targeted overproductions. PLoS Comput Biol 2010;6.
[45] Kim J, Reed JL. OptORF: optimal metabolic and regulatory perturbations for metabolic engineering of microbial strains. BMC Syst Biol 2010;4.
[46] Gu C, Kim GB, Kim WJ, Kim HU, Lee SY. Current status and applications of genome-scale metabolic models. Genome Biol 2019;20:121.
[47] Kumar A, Suthers PF, Maranas CD. MetRxn: a knowledgebase of metabolites and reactions spanning metabolic models and databases. BMC Bioinform 2012;13.
[48] Nazem-Bokaee H, Yen JY, Athamneh AIM, Apte AA, McAnulty MJ, Senger RS. SyM-GEM: a pathway builder for genome-scale models. Adv Biochem Biotechnol 2017;2:141.
[49] King ZA, Lu J, Drager A, Miller P, Federowicz S, Lerman JA, et al. BiGG Models: a platform for integrating, standardizing and sharing genome-scale models. Nucleic Acids Res 2016;44:D515–22.
[50] Pabinger S, Snajder R, Hardiman T, Willi M, Dander A, Trajanoski Z. MEMOSys 2.0: an update of the bioinformatics database for genome-scale models and genomic data. Database-Oxford; 2014.
[51] Karp PD, Billington R, Caspi R, Fulcher CA, Latendresse M, Kothari A, et al. The BioCyc collection of microbial genomes and metabolic pathways. Briefings Bioinform 2019;20:1085–93.
[52] Kanehisa M, Goto S. KEGG: kyoto encyclopedia of genes and genomes. Nucleic Acids Res 2000;28:27–30.
[53] Kanehisa M, Furumichi M, Sato Y, Kawashima M, Ishiguro-Watanabe M. KEGG for taxonomy-based analysis of pathways and genomes. Nucleic Acids Res 2023;51:D587–92.
[54] Arkin AP, Cottingham RW, Henry CS, Harris NL, Stevens RL, Maslov S, et al. KBase: the United States department of energy systems biology knowledgebase. Nat Biotechnol 2018;36:566–9.
[55] Henry CS, DeJongh M, Best AA, Frybarger PM, Linsay B, Stevens RL. High-throughput generation, optimization and analysis of genome-scale metabolic models. Nat Biotechnol 2010;28:977–82.

[56] Louis P, Galinski EA. Characterization of genes for the biosynthesis of the compatible solute ectoine from *Marinococcus halophilus* and osmoregulated expression in *Escherichia coli*. Microbiology 1997;143:1141–9.
[57] Caspi R, Altman T, Billington R, Dreher K, Foerster H, Fulcher CA, et al. The MetaCyc database of metabolic pathways and enzymes and the BioCyc collection of Pathway/Genome Databases. Nucleic Acids Res 2014;42:D459–71.
[58] Maruta K, Nakada T, Kubota M, Chaen H, Sugimoto T, Kurimoto M, et al. Formation of trehalose from maltooligosaccharides by a novel enzymatic system. Biosci Biotechnol Biochem 1995;59:1829–34.
[59] Thiele I, Palsson BO. A protocol for generating a high-quality genome-scale metabolic reconstruction. Nat Protoc 2010;5:93–121.
[60] Orth JD, Thiele I, Palsson BO. What is flux balance analysis? Nat Biotechnol 2010;28:245–8.
[61] Heirendt L, Arreckx S, Pfau T, Mendoza SN, Richelle A, Heinken A, et al. Creation and analysis of biochemical constraint-based models using the COBRA Toolbox v.3.0. Nat Protoc 2019;14:639–702.
[62] Valdes J, Pedroso I, Quatrini R, Dodson RJ, Tettelin H, Blake R, et al. *Acidithiobacillus ferrooxidans* metabolism: from genome sequence to industrial applications. BMC Genom 2008;9.
[63] De Smet KAL, Weston A, Brown IN, Young DB, Robertson BD. Three pathways for trehalose biosynthesis in *mycobacteria*. Microbiology 2000;146(Pt 1):199–208.
[64] Cardoso FS, Castro RF, Borges N, Santos H. Biochemical and genetic characterization of the pathways for trehalose metabolism in *Propionibacterium freudenreichii*, and their role in stress response. Microbiology 2007;153:270–80.
[65] Qu Q, Lee SJ, Boos W. TreT, a novel trehalose glycosyltransferring synthase of the hyperthermophilic archaeon *Thermococcus litoralis*. J Biol Chem 2004;279:47890–7.
[66] Kobayashi K, Kato M, Miura Y, Kettoku M, Komeda T, Iwamatsu A. Gene analysis of trehalose-producing enzymes from hyperthermophilic archaea in *Sulfolobales*. Biosci Biotechnol Biochem 1996;60:1720–3.
[67] Kouril T, Zaparty M, Marrero J, Brinkmann H, Siebers B. A novel trehalose synthesizing pathway in the hyperthermophilic *Crenarchaeon Thermoproteus* tenax: the unidirectional TreT pathway. Arch Microbiol 2008;190:355–69.
[68] Mamani S, Moinier D, Denis Y, Soulère L, Queneau Y, Talla E, et al. Insights into the quorum sensing regulon of the acidophilic *Acidithiobacillus ferrooxidans* revealed by transcriptomic in the presence of an acyl homoserine lactone superagonist analog. Front Microbiol 2016;7:1365.
[69] Cárdenas JP, Quatrini R, Holmes DS. Genomic and metagenomic challenges and opportunities for bioleaching: a mini-review. Res Microbiol 2016;167:529–38.
[70] Jung H, Inaba Y, Banta S. Genetic engineering of the acidophilic chemolithoautotroph *Acidithiobacillus ferrooxidans*. Trends Biotechnol 2021;40(6):677–92.